INSTITUTE FOR SPACE STUDIES

EVOLUTION OF O STARS. III. HELIUM BURNING

Richard Stothers

GODDARD SPACE FLIGHT CENTER

NATIONAL AERONAUTICS AND SPACE ADMINISTRATION

EVOLUTION OF O STARS. III. HELIUM BURNING

Richard Stothers

Institute for Space Studies
Goddard Space Flight Center, NASA
New York, N.Y.

ABSTRACT

12865

The evolution of a star of 30 $M_\odot$ is considered during the phases of helium ignition (I), depletion (He), and exhaustion (X).

After the brief I-phase (1.5×10^4 years) during which the onset of helium burning halts the gravitational contraction in the core, helium is depleted in a large convective region growing outward in mass fraction until it nearly overtakes the hydrogen burning shell. Helium depletion causes a radius shrinkage until $Y_c = 0.3$, whereupon the radius re-expands. The final C^{12}/O^{16} ratio in the core is uncertain, but will be zero if the critical reduced alpha width in O^{16} is greater than 0.3. The luminosity of the hydrogen shell source is low and monotonically decreases, even though the shell finally reaches the hydrogen-rich semi-convective zone ($\Delta X = 0.15$) when $Y_c = 0.01$. The star covers the spectral range from B1 to B8, while semi-convection maintains the total luminosity at a nearly constant value. The lifetime of the He-phase is 5.2×10^5 years.

Author

During the X-phase (1.3×10^4 years), the carbon-alpha reaction is able to sustain the luminosity in the shrinking convective core until $Y_c = 10^{-4}$. Thereupon the gravitational contraction in the core dominates the nuclear sources, and rapidly (10^3 years) brings the star into the region of late-type supergiants. The weak shell burning, prolonged by hydrogen enrichment due to full convective mixing at the inner boundary of the semiconvective zone, will then be extinguished by the envelope expansion. Since the new convective zone (along with the semiconvective zone) eventually retreats toward the surface, leaving behind a radiative zone of frozen composition, two major fixed composition discontinuities occur in the star: hydrogen-helium ($q = 0.44$) and helium-oxygen ($q = 0.37$).

The evolutionary features of very massive stars are discussed generally, and a time scale computed for the very late phases with and without neutrino emission. In either case, the total lifetime to iron core formation will be slightly less than 6 million years.

I. INTRODUCTION

The evolution of massive stars during the advanced phase of helium burning is not well known. Among the stars with $M > 10\ M_\odot$, this phase has been studied only in the case of $15\ M_\odot$ (Iben 1964) and $15.6\ M_\odot$ (Hayashi, Jugaku, and Nishida 1959, 1960; Hayashi and Cameron 1962; Hayashi, Hoshi, and Sugimoto 1962). The present paper considers in detail the evolution of a very massive star of $30\ M_\odot$ from helium ignition through exhaustion of central helium, and sketches briefly the more advanced phases up to iron core formation. It is a continuation of calculations on the previous phases (Papers I and II, Stothers 1963b, 1964).

II. ASSUMPTIONS

We adopt the same general assumptions of Papers I and II, including the complete mixing of material in convective regions and the absence of overshooting at the boundaries of convective and semiconvective regions. The distribution of energy sources is more complicated, however, as will be discussed in the next section. In conformity with the previous calculations, the opacity is assumed to be due only to

electron scattering, and the equation of state is represented by the sum of the perfect-gas and radiation pressure. The core is found to remain non-degenerate.

The age-zero chemical composition, retained by the outer radiative envelope, is again taken to be

$$X_e = 0.70, \quad Y_e = 0.27, \quad Z_e = 0.03, \quad X_{CNO} = Z_e/2. \tag{1}$$

III. GENERAL STRUCTURE

The overall structure of a very massive star is different in each of the evolutionary phases considered in this paper. We isolate three phases, as follows.

1. Helium ignition.—As the gravitational contraction of the core following central hydrogen exhaustion proceeds to raise the core temperature, helium burning begins near the center. The mass of the tiny convective region stops shrinking and increases again. Very quickly helium burning halts the gravitational contraction entirely, but the hydrogen shell source is still required to maintain the total luminosity.

2. Helium depletion.—During this phase helium is depleted in a large convective core growing out in mass fraction. Since the time scale is long compared with the previous phase, hydrogen depletion in the shell is also significant, and the mass fraction of the shell peak increases. Toward the end of central helium burning the shell reaches the semiconvective zone and burns at its inner boundary.

3. Helium exhaustion.—As the helium content of the convective core drops below 1 per cent, gravitational contraction again begins to play an important role. The contraction is further accelerated because of incipient photoneutrino emission. Having attained a maximum mass, the convective core now begins to retreat and leaves behind a region composed chiefly of oxygen. The hydrogen shell source continues to burn very weakly. As the total luminosity increases, the innermost part of the semiconvective zone becomes fully convective.

We adopt the following system of notations to designate the stellar zones, as closely in accordance with the notations of Papers I and II as possible: (I) the homogeneous outer

radiative envelope retaining the age-zero chemical composition, (IIa) the semiconvective intermediate zone, (IIb) the convective intermediate zone, (IIIa,b,c) the radiative intermediate zones, (IV) the convective core. Zones IIIa, IIIb, and IIIc are separated by the hydrogen-helium and helium-oxygen discontinuities, respectively. The following subscripts are also adopted: 1 for the Interface I-II, 2 for the inner boundary of Zone IIa, 3 for the outer boundary of Zone III, and 4 for the Interface III-IV. The hydrogen-helium discontinuity (hydrogen burning shell) will be designated by a subscript s. Thus for a semiconvective shell, $q_s = q_2 = q_3$, whereas for a convective shell, $q_s = q_3$. The helium-oxygen discontinuity will be designated by a subscript α. Thus for the outward-growing convective core, $q_\alpha = q_4$. Quantities referring to the immediately preceding evolutionary model will be marked with an $_t$.

The successive evolutionary phases will be denoted: I (helium ignition), He (helium depletion), and X (helium exhaustion), followed by a number indicating the particular model in the phase. Figure 1 represents the stellar structure in the phases considered in this paper.

Values of solar luminosity and radius were taken from Allen (1963), whereas in Papers I and II Chandrasekhar's (1939) values were used.

IV. ENERGY RATES

a) Nuclear Energy

Throughout all phases considered in this paper, the temperature of the hydrogen burning shell does not differ significantly from 5×10^7 ° K, so that we may use the following interpolation formula for the rate of the CNO-cycle:

$$\varepsilon_H = \varepsilon_H^o X X_{CNO} \rho T^\nu, \qquad (2)$$

with $\nu = 14$ and $\log \varepsilon_H^o = -99.0$. We assume the full equilibrium abundance of oxygen.

Below the hydrogen shell, C^{12} and O^{16} will certainly have reached their equilibrium abundances by the end of the hydrogen burning phase. Hence $X_N/X_{CNO} \approx 0.96$ or $X_N \approx 0.015$. By the onset of helium burning most of the N^{14} will have been destroyed by the reaction $N^{14} + He^4 \rightarrow O^{18}$, except for

a small amount of N^{14} mixed down as the convective core moves outward. Consequently, the initial abundances in the core for the main phase of helium burning are assumed to be

$$Y = 0.97, \quad X_{CN} = 0, \quad Z = 0.03, \tag{3}$$

and at first the nuclear energy generation of the core will be due to the triple-alpha reaction. For simplicity, we also neglect the contribution from nitrogen burning in the helium ignition phase.

When C^{12} is formed by the triple-alpha reaction, the C^{12} reacts with He^4 to form O^{16}. Subsequent alpha particle captures by O^{16} and O^{18} produce small amounts of neon and magnesium. However, from the calculated models, it may be estimated (Reeves 1964) that the final abundances will be less than about 5 per cent for Ne^{20} and Mg^{24}. Consequently, we are justified in considering the energy generation as due chiefly to the helium and carbon reactions. Reeves (1965) gives the energy generation rates as

$$\varepsilon_{He} = 3.45 \times 10^{11} \, f \, Y^3 \rho^2 \, T_8^{-3} \times 10^{-18.9/T_8}, \tag{4}$$

$$\varepsilon_C = 2.65 \times 10^{27} f X_C Y \rho T_8^{-2} \left(1 - 0.004 T_8 + 0.2 T_8^{-2/3}\right)^{-2} \times 10^{-\delta}, \quad (5)$$

where

$$\delta = 30.05\, T_8^{-1/3} + 0.06\, T_8^{2/3} \left(1 - 0.067\, T_8^{1/3}\right), \quad (6)$$

for the reactions $3\ He^4 \rightarrow C^{12}$ and $C^{12} + He^4 \rightarrow O^{16}$, respectively. Here $T_n = T \times 10^{-n}$. The weak electron screening correction applies at the densities of our models, and is given by (for both reactions)

$$f = 1 + 2.4\, \rho^{1/2} T_6^{-3/2}. \quad (7)$$

For simplicity we assume that f = 1. Afterwards, with the help of the calculated models, our assumption may be justified by showing that f is close to unity.

The reduced alpha width, θ_α^2, of the 7.12 Mev level in O^{16} is still very uncertain. We have used $\theta_\alpha^2 = 0.1$ with a possible error of a factor 10. Fowler and Hoyle (1964) give arguments for a rather large value of 0.78. We shall later investigate the effects of altering the value of θ_α^2, which enters the rate as a straight multiplicative factor.

b) Gravitational Energy

The rate of energy release due to gravitational contraction in the core is given by (Paper II)

$$\varepsilon_g = \frac{3}{2}\frac{kT}{\mu H}\left[\frac{\partial}{\partial\tau}\ln\left(T y^{-2/3} e^{-8y/3}\right) + \frac{5+8y}{3}\frac{\partial}{\partial\tau}\ln\mu\right], \qquad (8)$$

where $y = (1-\beta)/\beta$ and the time derivative applies to a given mass fraction.

c) Neutrino Emission

During helium exhaustion, neutrino losses begin to become important in dissipating energy from the star. The only process operative in our low-density models will be photoneutrino emission, $\gamma + e^- \rightarrow e^- + \nu + \bar{\nu}$. The rate is given by (e.g. Reeves 1965)

$$\varepsilon_\nu = 5\times10^7\ T_9^8\ . \qquad (9)$$

V. BASIC EQUATIONS

The basic equations for the stellar structure are given by equations (5) - (15) of Paper I. However, during the present phases L(r) is not constant outside the convective core. Therefore in equations (11) we replace the envelope parameter C by C' = Cw, where w = L(r)/L. The formulas for the various sources of luminosity are given below.

a) Shell Luminosity

Let the energy generation rate be represented by equation (2), and consider the shell source thin, with a peak at q_s and with X = 0 below q_s. Analogously to the procedure of Hayashi and Cameron (1962), we write

$$X = a_0 + a_1 q + a_2 q^2, \tag{10}$$

$$\rho T^{\nu} = \rho_s T_s^{\nu} \left(q/q_s\right)^{-\gamma}, \tag{11}$$

$$\gamma = -\left(\frac{\partial \log \rho}{\partial \log q}\right)_s - \nu \left(\frac{\partial \log T}{\partial \log q}\right)_s = \left(\frac{n+\nu}{n+1}\,\frac{V}{U} - \frac{d \log \mu\beta}{d \log q}\right)_s. \tag{12}$$

Now we may integrate ε_H to obtain

$$L_H = M\int_{q_s}^{1} \varepsilon_H \, dq = \varepsilon_H^o \, M \, q_s \rho_s T_s^{\nu} \left(\frac{a_o}{\gamma-1} + \frac{a_1 q_s}{\gamma-2} + \frac{a_2 q_s^2}{\gamma-3} \right). \quad (13)$$

In the radiative intermediate hydrogen zone, the composition gradient is frozen, so that the coefficients of equation (10) remain constant. In the semiconvective zone the composition gradient is continually changing, but is much less steep than in the radiative zone; therefore we set $X = X_s = a_o$ with little loss of accuracy. In the convective intermediate zone, $X = X_s$ exactly. The exponent γ is evaluated at q_s:

$$\gamma = \lambda + \frac{V}{U}\left[\frac{n+\nu}{n+1} + \frac{1-\beta}{\beta}\,\frac{n-3}{n+1}\right], \qquad \text{(radiative)} \quad (14)$$

$$\gamma = \frac{V}{U}\left[\frac{\nu}{(n+1)_{rad}} + \frac{1}{\Gamma_1}\right], \qquad \text{(semiconvective)} \quad (15)$$

$$\gamma = \frac{V}{U}\left[\frac{\nu}{(n+1)_{ad}} + \frac{1}{\Gamma_1}\right], \qquad \text{(convective)} \quad (16)$$

where $\lambda = d \log \mu / d \log q = (5/4)\,\mu\,(a_1 q + 2a_2 q^2)$. Beyond q_s, we assume no energy sources, so that here $w = 1$.

b) Nuclear and Neutrino Core Luminosity

Let the nuclear and neutrino energy rates be expressed in the following form,

$$\varepsilon = K_0 \rho^{\omega} T^{\nu}, \tag{17}$$

where ν will be a function of the central temperature, except in the case of the photoneutrino loss. Then, generally,

$$\begin{aligned} L &= \int_0^{M_4} \varepsilon \, dM(r) \\ &= K_0 \left(\frac{\mu_e H G}{k}\right)^{\nu} \frac{M^{\nu+\omega+1}}{(4\pi)^{\omega} R^{\nu+3\omega}} \left(\frac{x_4}{x_4^*}\right)^3 \left(\frac{\rho_4}{\rho_4^*}\right)^{\omega+1} \left(\frac{t_4}{t_4^*}\right)^{\nu-\omega-1} \\ &\quad \times l_c^{\omega+1} \int_0^{x_4^*} (\beta\rho^*)^{\omega+1} t^{*\nu-\omega-1} x^{*2} \, dx^*. \end{aligned} \tag{18}$$

In particular, we have the following cases:

$$\begin{array}{lccc} L = & L_{He}, & L_C, & L_\nu, \\ \omega = & 2, & 1, & 0, \\ K_0 = & \varepsilon^0_{He} \rho Y^3, & \varepsilon^0_C \rho X_C Y, & \varepsilon^0_\nu. \end{array} \tag{19}$$

c) Gravitational Luminosity

Energy release due to gravitational contraction is assumed to occur below the hydrogen-helium discontinuity where the hydrogen burning shell is located. This assumption is later justified by the detailed calculations. From the results of Paper II the rate of gravitational energy release is approximately independent of mass fraction. Consequently we have

$$L_g = \varepsilon_g M (q_s - q_4), \qquad \text{(I-phase)} \qquad (20)$$

$$L_g = \varepsilon_g M q_g . \qquad \text{(X-phase)} \qquad (21)$$

In the case of the I-phase, it is found that the steep temperature dependence of the helium burning rate allows the nuclear source to sustain the convective core against its gravitational contraction. Thus we assume that gravitational energy release occurs only in the dehydrogenized, non-helium-burning Zone IIIb. For the X-phase, q_g is chosen to be q_s or q_α, as discussed in Section XI.

VI. INTEGRATION METHOD

With trial envelope parameters (to be specified below), Zones I - IV are integrated from the surface inward to the point in Zone IV where the conditions $U < 3$ and $dU/dq < 0$ are no longer fulfilled. Revision of the trial parameters is made until these conditions are met at some prechosen mass fraction close to the center. Then a starting value for β_c is extrapolated, so that outward and inward integrations may be performed. Fitting is made in U and V at a specified β_f just inside Zone IV.

VII. NUCLEOSYNTHESIS

As hydrogen is consumed in a shell, the mass fraction of the shell moves outward at a rate given by

$$\frac{\Delta \int X \, dq}{\Delta \tau} = - \frac{L_H}{M E_H} , \tag{22}$$

where $E_H = 6.0 \times 10^{18}$ erg/gm and

$$-\Delta \int X \, dq = \int_{q_s'}^{1} X_i \, dq - \int_{q_s}^{1} X \, dq . \tag{23}$$

In the helium burning core, the time rates of change of He^4, C^{12}, and O^{16} are given by

$$\frac{\partial Y}{\partial \tau} = -\frac{\epsilon_{He}}{E_{He}} - \frac{1}{3}\frac{\epsilon_C}{E_C}, \tag{24}$$

$$\frac{\partial X_C}{\partial \tau} = \frac{\epsilon_{He}}{E_{He}} - \frac{\epsilon_C}{E_C}, \tag{25}$$

$$\frac{\partial X_O}{\partial \tau} = \frac{4}{3}\frac{\epsilon_C}{E_C}. \tag{26}$$

Consequently, we may write for the core

$$\frac{\Delta \int Y dq}{\Delta \tau} = -\frac{L_{He}}{M E_{He}} - \frac{1}{3}\frac{L_C}{M E_C}, \tag{27}$$

$$\frac{\Delta \int X_C dq}{\Delta \tau} = \frac{L_{He}}{M E_{He}} - \frac{L_C}{M E_C}, \tag{28}$$

$$X_O = 1 - Z_e - Y - X_C. \tag{29}$$

Combination of equations (27) and (28) yields a quartic equation for Y.

VIII. UNSTABLE INTERMEDIATE ZONES

a) Semiconvection

In Paper I it was shown how the following criterion for convective instability,

$$(n+1)_{ad} \geq (n+1)_{rad} \Big/ \left\{1 - \frac{\beta}{4-3\beta} \frac{d\log\mu}{d\log P} (n+1)_{rad}\right\}, \qquad (30)$$

must be used in a chemically inhomogeneous region. The equality sign in this criterion is used to determine the distribution of chemical composition that is actually set up by mixing in an unstable zone, so that the zone attains a state of convective neutrality. This mixing phenomenon is called semiconvection.

Since the upper boundary of the semiconvective zone (q_1) merges smoothly into the outer radiative zone, the material here is nearly homogeneous; consequently, any convective instability is uninhibited at q_1. At the lower boundary ($q_2 = q_3$) the steepening gradient of mean molecular weight eventually chokes off the convective motions. Thus, in the early models during the hydrogen-burning phase, the zone below q_2 is actually radiative even though $(n+1)_{ad} > (n+1)_{rad}$.

These considerations remove the apparent contradiction found by Savedoff and van Dyck (1959), who neglected the term in $d\ell n\mu/d\ell nP$ in equation (30).

The effect of semiconvection on the stellar evolution was shown to be small during the phases considered in Papers I and II. In fact, the effect is completely negligible throughout the hydrogen burning phase, since the following conditions are <u>both</u> satisfied at the same mass fraction ($q_2 = q_3$):

$$U_3/U_2 = V_3/V_2 = \mu_3/\mu_2, \tag{31}$$

$$\int_{q_2}^{1} X_{II}\, dq = \int_{q_3}^{1} X_{III}\, dq. \tag{32}$$

Hence for computational purposes, it was sufficient to consider the intermediate zone of inhomogeneous composition as wholly radiative. Eventually, however, the growing semiconvective zone makes itself felt by slightly changing the values of the physical variables in the inner radiative zone (but not the chemical composition which remains frozen) from those values that would obtain if the semiconvective zone

were assumed radiative. This effect shows up when conditions (31) and (32) are not simultaneously or individually satisfied. By the onset of helium burning, condition (32) is satisfied at a mass fraction that is several per cent smaller than q_2. Computationally, we now integrate the semiconvective zone directly from q_1, applying the jump in chemical composition (eq. [31]) when condition (32) is met. The jump in μ to the frozen value of μ in the radiative zone automatically produces the proportionate jump in U and V. This was not the case before, since U_3 and V_3 depended on the integration of the assumed radiative zone.

b) Full Convection

When the inner boundary of the semiconvective zone reaches the dehydrogenized helium zone, condition (32) is replaced by the condition that hydrogen be conserved: $\Delta\int X dq = 0$. As the luminosity continues to increase, it eventually becomes impossible to satisfy this condition beyond a certain q_m, denoting the maximum inward extent of the semiconvection. A new mechanism must be found to maintain a downward transport of hydrogen. Apparently the only selfconsistent scheme involves the growth of a fully

convective region between the semiconvective zone and the radiative helium zone. In this scheme the semiconvective zone retreats with sufficient helium enrichment to maintain convective neutrality, while the growing convective region steadily drains hydrogen and helium from its inner boundary. The net effect is to increase the hydrogen content of the homogeneous convective region, since the semiconvective zone is always relatively richer in hydrogen.

With modest increases in the luminosity, the inner boundary of the convective region moves very slightly inward of q_m. As a good approximation, we assume composition discontinuities at the inner (q_3) and outer (q_2) boundaries of the region. At these boundaries it is necessary that $(n+1)_{rad} = (n+1)_{ad}$, in order to preserve continuity of the radiative flux. This condition of equality, in fact, determines the amount of composition jump at q_2, since $(n+1)_{rad} < (n+1)_{ad}$ for $q_2 < q < q_1$. Finally, we require that hydrogen be just conserved when $(n+1)_{rad} = (n+1)_{ad}$ at q_3.

By the end of helium exhaustion, the inner boundary of the convective region begins to move outward. It is found

that a new radiative zone is left behind. Hence, both the semiconvective and fully convective regions start to approach the stellar surface. Within the new radiative zone left behind, the composition gradient is determined by $\ell = \ell_s (q/q_s)^{-\lambda}$, analogous to the gradient left behind by the shrinking convective core during hydrogen burning (Paper I). However, in the present case, λ can be directly determined by use of ℓ_3 and ℓ_m. Thus for either an inward- or outward-moving convective region, q_2 is the only unknown, which must be solved for by trial and error until the condition of hydrogen conservation is met.

IX. HELIUM IGNITION PHASE

In this phase we adopt a run of chemical composition throughout the star as shown in Table 1. The hydrogen abundance in the radiative intermediate Zone IIIa is given by

$$X = -1.085 + 3.830\, q - 1.43\, q^2. \qquad (33)$$

This is the distribution found in the last model of the gravitational contraction phase following hydrogen exhaustion (Paper II). However, we now assume that X = 0 below an infinitely thin shell source at q_s. The effect of an abrupt change of X at q_s through κ and μ is not large if X_s is small. Since the time scale of the helium ignition phase is short, we further assume that hydrogen depletion in the shell source is negligible; thus q_s will remain constant. From Paper II, the peak of the shell source is at $q_s = 0.328$. It is found that the models during the brief I-phase of unchanging chemical composition are not very sensitive to the particular value of q_s; therefore we have chosen the shell peak of Model G6, at which $X_s = 0.018$.

Integration of models for this phase is performed as follows. First, the evolutionary step is taken by specifying C. Since gravitational contraction is assumed to occur only in Zone IIIb, the non-dimensional luminosity in this zone is given by

$$w = 1 - w_s - (q_s - q)\, w_g^* , \tag{34}$$

where $w_g^* = w_g/(q_s - q_4)$. Trial integrations are then performed with a fixed value of w_g^*, for various values of w_s until a fitted model is obtained. The fitted model yields q_4 and hence w_g. Substitution of the non-dimensional variables of Paper I (eqs. [8] and [10]) into equation (13) gives a relation between w_s and R, which then determines the physical variables. Since no significant depletion of the helium occurs, nuclear burning in the core is due only to the triple-alpha reaction. Hence the nuclear core luminosity may be calculated from equation (18), yielding an implied value for the gravitational luminosity, $w_g' = 1 - w_s - w_{He}$. A new value of w_g^* is obtained from w_g' and q_4, and the whole procedure is iterated until $w_g = w_g'$.

The time step, $\Delta\tau$, is computed from equation (18) by using equation (20) to obtain ε_g and by evaluating the physical variables at a point midway between q_s and the mean value of the present and previous q_4. For the I-phase only, the semiconvective zone was treated in the manner described in Paper I.

Table 2 gives the results for six models representing the helium ignition phase. The first model corresponds to

a stage only slightly more advanced than the last stage in Paper II. After a brief time, the steep temperature dependence of the helium burning rate ($\nu \approx 20$) allows helium burning to sustain the entire dehydrogenized zone by only a very slight increase in T_c and ρ_c. The convective core grows extensively in mass fraction as a consequence. Although the computed time steps are rather rough, it is estimated that hydrogen depletion in the shell corresponds to an equivalent change in q_s of only 0.01. As we have noted above, the structure will not be sensitive to q_s; therefore neither will be $\Delta\tau$. The total time elapsed between the onset of helium burning at the center and cessation of the core gravitational contraction is about 1.5×10^4 years.

X. HELIUM DEPLETION PHASE

During the main phase of helium burning, the only energy sources are nuclear: helium and carbon burning in a convective core and hydrogen burning in a thin shell. The distribution of chemical composition is given by Table 1 and equation (33). Since the time scale of the He-phase is

long, nuclear burning in the shell depletes a significant amount of hydrogen and causes q_s to increase (Fig. 2a). In the convective cone, helium burns into carbon and oxygen. However, the resulting composition discontinuity at the boundary of the outward-moving core will not violate the condition of continuity of radiative flux at non-nuclear burning interfaces (Paper I), since the electron scattering opacity is constant in a dehydrogenized region.

In the numerical integrations, the evolutionary step is taken by specifying q_s. With fixed values of C and (Y, X_C) at the center, trial integrations are run with various values of w_s until a fitted model is obtained. As in the I-phase, equation (13) determines R and thus all the physical variables. The core luminosity is then obtained from equation (18) and gives an implied value for the shell luminosity, $w_s' = 1 - w_{He} - w_C$. Comparison of w_s and w_s' yields an improved guess for C. The procedure is iterated until $w_s = w_s'$ for some value of C. Then the time step, $\Delta\tau$, is computed from equation (22), using the amount of hydrogen depletion, $\Delta\int Xdq$, between q_s' and q_s. The choice of q_s for the initial model is not critical, because X_s is small over

a large range in mass fraction near $q_s = 0.328$. Improved values of (Y, X_c) are obtained by solving equations (27) and (28). Finally, the whole scheme may be iterated to obtain the definitive values of C and (Y, X_c).

For the He-phase, the semiconvective zone was treated explicitly, as described in Section VIII. Its effect may be assessed by comparing the initial model for this phase (Table 3) with the final model for the previous phase (Table 2), where the semiconvective zone was assumed radiative. Both models represent the same stage. The effect is chiefly a slight lowering of the luminosity and a relative increase in the central condensation. The lower luminosity is due to the indirect effect of the hydrogen discontinuity at q_2. This discontinuity steepens the radiative temperature gradient, $dT/dr \sim \varkappa\mu \sim (1+X)^{-0.4}$, beyond what it would be in the assumed radiative case for the same luminosity. Consequently, the shell temperature becomes too high, causing $L_H \sim T_s^{\nu}$ to run away. The shell temperature may be reduced only by decreasing dT/dr, hence by shrinking the hydrogen discontinuity (and therefore the extent of semiconvection). Consequently, the total

luminosity must be lower in the semiconvective case. On the other hand, the relative increase in central condensation, $U^{-1} \sim \mu^{-1}$, is caused chiefly by the hydrogen enrichment of the inner envelope caused by semiconvection.

When the shell source consumes its way to the semiconvective zone, ΔX is only 0.15 at the interface (Fig. 2a). Thus the sole effect of the encounter is a slight prolongation of shell burning, by which L_H remains temporarily constant. The reason for the convective instability just outside the shell lies essentially in the steepening temperature gradient there. As pointed out in Paper II, $(n+1)_{ad}$ approaches $(n+1)_{rad}$ as β_s decreases. However, in the present case, the decrease in β_s is due to the increase in $\varkappa \sim 1+X$ as the shell moves outward, since the total luminosity remains nearly constant during helium burning. This may be seen by observing that $(1-\beta)/\varkappa L \sim (n+1)_{rad} \approx (n+1)_{ad} \approx$ constant.

For a wide range of stellar masses, the radius begins to expand when $Y_c = 0.3$ (cf. 4 $M_\odot$ and 15.6 $M_\odot$ in Hayashi, Hoshi, and Sugimoto 1962). Since the nuclear burning rate goes as Y^3 for helium burning, as opposed to X for hydrogen

burning, the value $Y_c = 0.3$ corresponds to that value $X_c = 0.03$ at which the radius changes direction during hydrogen burning. When Y_c is as low as 1 per cent, the star still has a radius characteristic of an early-type supergiant. The reason is essentially that the nuclear core luminosity is enabled to continue increasing by carbon-alpha burning at high temperature (see Sec. XII).

In order to maintain the high luminosity, β_c remains low. We note that β_c is lower at the end of helium burning than at the end of hydrogen burning. This produces the more extensive convective core in the present case. By Model He10, the core size has reached its maximum extent, only 0.07 in mass fraction below the hydrogen shell source (Fig. 2b). The low value of β_c also keeps the ratio ρ_c/T_c^3 small. Since nuclear reactions not only sustain the core but expand it slightly during the early stages of helium burning, ρ_c tends to remain very low. Consequently, T_c is high in order to maintain the appropriate nuclear reaction rate. It is because of these relatively higher temperatures in the cores of massive stars that the carbon-alpha reaction (which occurs at a higher temperature than

the triple-alpha process) is able to get under way before all the helium is burned into carbon.

The products of the carbon-alpha reaction depend critically on an uncertain reduced alpha width in O^{16}, as discussed in Section IV. With our adopted value of $\theta_\alpha^2 = 0.1$, the core is still composed of one-third unburned carbon (by mass) at the end of helium burning. Calculations based on the model parameters of Table 3 indicate that the composition of the core will be all oxygen and heavier elements if θ_α^2 exceeds 0.3.

XI. HELIUM EXHAUSTION PHASE

In this phase, gravitational contraction in the core gradually replaces helium burning as the source of energy, when the abundance of helium drops below 0.01 by weight. The core composition does not change significantly, and in view of the uncertainty of the final products, we have simply adopted $\mu = 2$ below $q = 0.371$, the maximum extent of the convective core (Model He10). The helium discontinuity at $q = 0.371$ (Fig. 2b) represents the location of the helium shell, which is not ignited during the stages

considered here. Hydrogen depletion in the outer shell is negligible on account of the short time scale involved; therefore q_s is determined by the convective instability, as discussed in Section VIII. Table 1 illustrates the run of chemical composition throughout the star. It does not change appreciably during this phase.

Since the gravitational contraction rate is not uniform between the composition discontinuities ($q_\alpha < q < q_s$), we have constructed two sequences of models, with $q_g = q_s$ and $q_g = q_\alpha$, as extreme cases bracketing the true models. Model construction proceeds as in the helium ignition phase (Sec. IX), except that we assume here gravitational contraction occurring uniformly throughout the whole region below q_g and a central nuclear burning due only to the carbon-alpha reaction (minus photoneutrino emission). Hence we substitute $w_g^* = w_g/q_g$ into equation (34) and compute $w_g = 1 + w_\nu - w_s - w_C$. The time step, $\Delta\tau$, may in the present case be evaluated at the center of the star, and our guessed values for (Y, X_C) in the convective core improved, as for the helium depletion phase. A sufficiently accurate expression for the time scale may be approximated from equation (8):

$$\Delta\tau = \frac{3}{2}\,\frac{k}{\mu_c H}\,\frac{\Delta T_c}{\varepsilon_g}\,. \tag{35}$$

The neglect of $\Delta\mu_c$ in the early stages will not be serious since ε_g is small. Furthermore, β_c remains nearly constant so that we may also neglect Δy_c.

The results for the X-phase are displayed in Table 4. The assumption of $q_g = q_s$ or $q_g = q_\alpha$ leads to significantly different temperatures and fractional luminosities at the tabulated stages. Consequently, only rough values of the radius and effective temperature are given.

During the onset of the X-phase the region just outside the hydrogen discontinuity at the shell becomes fully convective, mixing down additional hydrogen and prolonging shell burning (Fig. 2a). The boundary at $q_s = q_3$ remains remarkably constant for moderate changes in the luminosity, although there is indication of a slight decrease. Eventually, however, when the increasing central condensation necessitates an even higher luminosity, the convective intermediate region moves out as a whole toward the surface, continuing to penetrate the semiconvective zone but leaving behind a new radiative zone of frozen composition (Fig. 2a).

The inner boundary of this new Zone IIIa is thus fixed at $q_s = 0.439$ with $X_s = 0.528$.

When β_c is stabilized as the gravitational luminosity increases, the convective core shrinks in mass fraction. The final products of nuclear burning are deposited in a radiative zone left behind by the retreating convective core. As we have seen, this nuclear ash will be predominantly carbon and/or oxygen. The exhaustion of nuclear fuel takes place on a gravitational time scale, similar to that computed for the I-phase, about 1×10^4 years. Of this, only 10^3 years are required to cross the Hertzsprung Gap. It is uncertain whether helium will be completely exhausted from the inner core before or after this crossing; however, nuclear burning in the core is found to become negligible when $T_c = 3.7 \times 10^8$ ^oK and $\rho_c = 2800$ gm/cm^3. At this point photoneutrino emission will contribute 3 per cent of the luminosity.

The internal evolution of the star is displayed in Figure 1, from the onset of helium burning through its exhaustion at the center.

XII. EVOLUTIONARY FEATURES

In this section a general exposition of the basic features in the evolution of very massive stars from main sequence dwarfs to red supergiants will be essayed. Hayashi, Hoshi, and Sugimoto (1962) and Stein (1965) have discussed the stars of lower mass in similar detail. In particular, the evolutionary history of the stellar center, surface, and energy-producing regions may be used to summarize a star's total evolution. We shall investigate each of these points in turn for the case of a star of 30 $M_{\odot}$.

a) Center

The evolution of the stellar center is shown on a log ρ - log T diagram in Figure 3. It is of particular interest to note that the dotted curve of calculated models follows closely a line of slope 3, representing Lane's law of homologous evolution: β_c = constant. The major deviations occur during the early phases of nuclear burning (both hydrogen and helium) when the core expands slightly. The slight veering toward isothermal evolution is apparent during the gravitational contraction phases. These deviations,

however, are small when we compare them with the deviations occurring for a star even as massive as 15.6 $M_\odot$ (Hayashi and Cameron 1962, Fig. 6). The reason is the extremely low densities and high mass, which minimize effects such as electron degeneracy and isothermality.

b) Surface and Shell Source

In Paper II an interpretation of the envelope expansion was given in terms of the chemical inhomogeneity and the U-V plane. We noted that $V \to 4$ and $U \to 0$ as $r \to 0$ in a polytropic envelope of index $N = 3$. Since the rising luminosity in our calculated envelopes centrally condenses the models and increases the mean effective polytropic index toward $n = 3$ (on account of decreasing β), the U-V curve shifts upward and to the left in Figure 4. Thus the increase in total stellar radius may be understood from the integration of $d \log r = U^{-1} \, d \log q$ (Hayashi, Hoshi, and Sugimoto 1962):

$$\log R = \text{constant} + \log (\mu_c T_c^{-1}) + \int_{q_s}^{1} U^{-1} \, d \log q . \qquad (36)$$

This relation gives an explanation of the general trend of radius expansion beyond the initial main sequence.

The fluctuations in radius were considered in Paper II in terms of the relative importance of radiation pressure. We showed that since, generally, $R \sim (1-\beta)^{1/2}/\beta T$ in a polytropic region, the shell radius and the total radius are governed mainly by β_c and β_s, respectively, for the core and envelope considered as two separate "polytropes". The results for the helium phases are in accord with this picture.

We shall now discuss further the radius fluctuations in terms of the stellar energy requirements and the effect of the hydrogen shell source. Therefore we trace the evolution from the onset of hydrogen exhaustion to the end of helium exhaustion. For completeness, however, we begin with a discussion of the initial hydrogen burning phase.

During this phase of hydrogen depletion in the core, the envelope expansion is due to the growing chemical inhomogeneity, which reduces U and increases μ_c (cf. eq. [36]). However, we note that in a completely mixed star, even though μ_c monotonically increases with time, the radius finally begins to shrink because the decrease in X_c

eventually outruns the increase in $\mu_c \sim (1+X_c)^{-1.4}$ (cf. eq. [16], Paper I).

In general, the rise of luminosity during hydrogen depletion in a star may be understood by the increase of mean molecular weight, through the rough relation $L \sim \mu^4$. More precisely, as hydrogen is consumed near the center, the energy flux expands the star, and the central temperature rises to offset the decreases in density and hydrogen content. The consequent steepening of the temperature gradient must then be maintained by an increasing luminosity, according to the radiative transport equation.

During the hydrogen exhaustion phase, gravitational contraction of the core helps to raise T_c (in accordance with the virial theorem) and hence T_s. However, since T_s and the time scale are much too small to displace q_s by nuclear burning, nowhere in the star does μ change significantly. Consequently, L remains nearly constant, thereby freezing the non-dimensional structure of the envelope. Because $R \sim T_c^{-1}$ for such a configuration, the whole radius shrinks. This behavior is similar to the evolution during the pre-main-sequence contraction phase.

During the brief gravitational contraction phase following hydrogen exhaustion, the accelerated central condensation produces a sudden rise in total luminosity. The reason for this is twofold. First, in stars of high mass, the large core cannot withstand an energetic gravitational contraction, so that a temperature gradient persists in it. Since this gradient steepens on account of the marked increase of T_c compared with T_s (because of the sensitivity of L_H to temperature), a suitably high luminosity in the core is required to support the gradient. Maintenance of such luminosity near the center leads to a higher total luminosity in the case of a gravitational source of energy, because ε_g is more uniform throughout the core than ε_H. Second, the gravitational infall of the shell raises its temperature and thereby augments the shell luminosity, too. Hence the whole stellar luminosity increases significantly.

In stars of low mass with isothermal cores less than the Schönberg-Chandrasekhar limit ($q = 0.1$), the luminosity is due almost entirely to shell burning; the increase of luminosity will then be due to the temperature rise at the shell, caused by slow contraction of the isothermal

core. In stars of all masses, however, the radius expansion can be ascribed to the marked increase of energy flow into the envelope.

During the early stages of helium burning when the time scale is long, nuclear burning in the shell causes a large increase of q_s. To compensate for the outward motion of the shell (which tends to reduce T_s) and the depletion of helium in the core (which increases μ), the central temperature continues to rise. Although the shell burning is consequently maintained in order to meet the total flux requirements, its luminosity drops gradually because of the slowly decreasing temperature. Hence the total luminosity of the star is merely kept at a constant value and not increased in accordance with $L \sim \mu^4$, as for a point convective source. To keep the shell burning at a sufficiently high temperature, the total radius must shrink. This may be seen simply from consideration of the frozen non-dimensional structure of the envelope (since L is nearly constant). As t_s decreases for larger q_s, R must also decrease in order to maintain $T_s \sim t_s R^{-1}$.

When q_s is stabilized in the later stages of helium burning (because of the short time scale due to low Y_c),

the gradual increase in luminosity expands the envelope. This expansion is reflected in the monotonic decrease of L_H (through lower T_s, which, because of the near constancy of t_s, implies an increased R). The deficiency of L_H is met by an increase in L_{core} caused by the growing mass fraction, q_4, of the convective core, which mixes down fresh helium. This is in contrast with the hydrogen exhaustion phase where q_4 (and consequently L_{core}) <u>decrease</u>. The total luminosity of the star now rises more noticeably as q_s remains nearly constant, in accordance with the trend indicated by $L \sim \mu^4$. However, since the helium content is already low, μ and therefore L do not change as much as during hydrogen burning.

During the helium exhaustion phase, the shell source supplies the small deficiency in the core luminosity. Thus the stellar structure behaves in a way more like the gravitational contraction phase following hydrogen exhaustion rather than the hydrogen exhaustion phase itself, in which the shell source and the chemical composition discontinuity were just being set up. Analogously, the luminosity rises and the radius expands. By the end of helium burning, the total luminosity is already so high that any small increase

produces a large central condensation of the envelope. This explains why, in very massive stars, the luminosity remains practically constant throughout helium burning (which resists central condensation), and thereafter produces a tremendous envelope expansion with only a moderately small brightening. The high luminosity also explains the complicated occurrence of convectively unstable regions in the envelope. In such convective regions the temperature gradient is practically fixed, so that the increasing temperature on the inside promotes expansion of the radius.

c) Convective Core

As nuclear fuel is ignited in the central regions of stars, a convective core is formed if either the temperature exponent of the energy generation rate or the radiation pressure $(1-\beta)$ is high enough. This convective core grows outward in mass fraction very rapidly at first, reaching a maximum extent, whereupon it subsequently retreats. However, its detailed behavior is very different if the nuclear energy is due to hydrogen or helium burning. In the case of hydrogen burning, maximum core extent occurs at the end of the pre-

main-sequence contraction, that is, when X_c is still equal to X_e. However, in the case of helium burning, it occurs at the onset of core contraction during helium exhaustion, when $Y_c \approx 0.01$. The difference in behavior is essentially caused by the electron scattering opacity, and therefore occurs only in stars where this opacity dominates.

The reasons may be seen in detail, as follows. The boundary of the convective core is defined as the point where $(n+1)_{rad} = (n+1)_{ad}$. From Paper I, we then have that

$$q_4 = \frac{0.19}{16\pi c G M} \left[\frac{1+X}{1-\beta} L(r) (n+1)_{ad} \right]_4 . \qquad (37)$$

Since the fractional change of $(n+1)_{ad}$ is small compared with the fractional changes of the other variables in equation (37), we may consider $(n+1)_{ad}$ as constant. Now, during the pre-main-sequence contraction phase, L and $1-\beta$ are approximately constant. However, $L(r_4)$ rises rapidly due to the onset of hydrogen burning near the center, the balance in L being supplied by the envelope contraction. Thus $q_4 \sim L(r_4)$, or q_4 increases.

Since hydrogen burning fully sustains the core during the H-phase, the density increase is halted, permitting $1-\beta$ to rise with temperature. Thus $L = L(r_4) \sim 1-\beta_4$ (roughly), with the result that $q_4 \sim \kappa_4 \sim 1 + X_4$. Hence during hydrogen depletion, the opacity decreases and the core mass shrinks. These considerations supplement those of Sakashita, Ôno, and Hayashi (1959), who showed that the convective core could at least not grow in mass.

Helium ignition in the core behaves in a similar way to hydrogen ignition, resulting in an increase of q_4. However, during the He-phase, the now constant opacity ($\kappa = 0.19$) does not regulate the core size as it did during the H-phase. Since the structure is altered by the presence of composition discontinuities and a shell source, it is also no longer true that $L(r_4) \sim 1-\beta_4$. In fact, $L(r_4)$ increases by a much larger factor than $1-\beta_4$ can. Hence $q_4 \sim L(r_4)/(1-\beta_4)$, or q_4 increases as helium is depleted.

During helium exhaustion, gravitational contraction in the core begins to replace the nuclear source of energy. Since the gravitational source is uniform and distributed well beyond the convective region, $L(r_4)$ decreases. The density rises considerably and checks the increase of $1-\beta_4$,

which, as during all gravitational contraction phases, remains roughly constant. Thus it is only at the end of helium burning that the convective core begins to shrink, on account of the decreasing luminosity at q_4.

XIII. LATE EVOLUTIONARY PHASES

Whether the high-temperature neutrino processes exist in nature or not, their inclusion in our models up to the end of helium exhaustion does not substantially jeopardize the results since the neutrino luminosity rises to only a few per cent of the photon luminosity at this stage. To calculate further a rough time scale of the ensuing evolutionary phases, we must discuss separately the cases of evolution with and without neutrinos. In both cases we assume that the initial core composition is pure oxygen.

a) Photonic Evolution

Under normal evolutionary conditions, gravitational contraction will heat up the core until oxygen burning sustains the structure. We assume that the gravitational

energy release, which is taken to be uniform throughout the core, may be represented by

$$\varepsilon_g = \frac{3}{2}\frac{k}{\mu_c H}\frac{\partial T_c}{\partial \tau} = \frac{dL(r)}{dM(r)} = \frac{L}{M}\frac{w_g}{q_g}. \qquad (38)$$

Solving for the time, we have

$$\tau = \frac{3}{2}\frac{kM}{\mu_c H}\frac{\Delta T_c}{L}\frac{q_g}{w_g}. \qquad (39)$$

Equation (39) will no longer be valid when $L_{nuc} \geq L_g$. This will happen when $\bar{\varepsilon}_{nuc} = \varepsilon_g$. If we assume a nuclear energy generation rate in the form of equation (17), then it may be shown for a polytrope of index 3 that (Reeves 1963)

$$\bar{\varepsilon}/\varepsilon_c = 2.4\,(\nu + 3\omega + 3)^{-3/2}. \qquad (40)$$

With $q_g = 0.4$, $w_g = 0.5$, $L = 10^6\ L_\odot$, and the evolutionary relation $\rho \sim T^3$, we obtain $T_c = 1.5 \times 10^9\ ^\circ K$ when $\bar{\varepsilon}_{nuc} = \varepsilon_g$. By using this final temperature and an initial temperature of $3.7 \times 10^8\ ^\circ K$, equation (39) yields $\tau = 3 \times 10^4$ years.

Thereafter, oxygen burning and successive gravitational contractions interrupted by still more advanced nuclear burning phases up to iron formation supply the stellar luminosity. Since the gravitational phases will be negligibly short compared with the nuclear phases, we consider only

$$\tau = EZMq_4/Lw_4 . \tag{41}$$

Oxygen burning will be the dominant nuclear phase. We estimate roughly that $Z = 1$, $q_4 = 0.3$, $w_4 = 0.5$, and $L = 10^6\ L_\odot$. With $E = 9 \times 10^{17}$ erg/gm for the conversion of oxygen into iron, we obtain $\tau = 3 \times 10^5$ years. Even if the initial core composition were pure carbon, the lifetime of the star as a red supergiant would not be substantially increased.

b) Neutrinic Evolution

On the assumption of neutrino emission, the longest of the late evolutionary phases will be the gravitational contraction following helium exhaustion, when the evolution

is at first primarily limited by photon radiation. Thus equation (39) will apply up to a certain temperature at which $\bar{\varepsilon}_\nu = \varepsilon_g$. This temperature may be calculated as above. With $w_g = 1$ and $L = 4 \times 10^5\ L_\odot$, we obtain $T_c = 6.1 \times 10^8\ ^\circ K$. Hence $\tau = 7 \times 10^3$ years.

At a temperature around $6 \times 10^8\ ^\circ K$, three changes in the stellar luminosity will take place. First, neutrino emission will predominate over the photon radiation. Second, photoneutrinos will be replaced by pair annihilation neutrinos as the dominant neutrino source. Third, the helium shell will be ignited. However, since the total photon luminosity will not rise very much in comparison with the increasingly powerful neutrino luminosity (Reeves 1963), the helium shell may be neglected.

The evolution of the star is thus limited only by the rate of neutrino emission from pair annihilation, that is, $L_\nu = L_g$. Under the assumption that $\rho \propto T^3$, the time scale is given by (Stothers 1963a)

$$\tau = \frac{3}{2} \frac{k}{\mu H} \Delta\left(\overline{\frac{T/\varepsilon_\nu}{n-4}}\right) . \qquad (42)$$

This yields $\tau = 6 \times 10^3$ years.

Oxygen burning may briefly sustain the neutrino losses at a temperature around 2×10^9 °K. For a polytropic core mass of 9 $M_\odot$, Reeves (1963) estimates the oxygen burning lifetime at 2 months or less. Subsequently, gravitational contraction must supply the neutrino losses while further nucleosynthesis up to iron formation takes place in the core, on a time scale of minutes. Thus the total lifetime from the end of helium exhaustion will be about 1.3×10^4 years, on the neutrino hypothesis.

XIV. PRE-MAIN-SEQUENCE CONTRACTION

Chandrasekhar (1939) has given an expression for the pre-main-sequence contraction time:

$$\tau = \frac{1}{5-N} \frac{3\gamma-4}{\gamma-1} \frac{GM^2}{LR} . \qquad (43)$$

If we assume for the ratio of specific heats $\gamma = 5/3$ and for the polytropic index $N = 3$, then equation (43) yields 2.3×10^4 years. The implicit assumption that L = constant is a good approximation for very massive stars. In fact, τ as deduced from equation (43) is reasonably close to values for 30 $M_\odot$ interpolated from the approximate models of Tanaka

and Sakashita (1965) and from the more exact models of Ezer and Cameron (1965).

XV. FINAL REMARKS

The time scale of evolution for the different phases of a 30 $M_\odot$ star is given in Table 5. The helium burning lifetime is one-tenth of the hydrogen burning lifetime; this fraction is somewhat larger than for 15.6 $M_\odot$ (Hayashi and Cameron 1962) because of the higher initial hydrogen abundance assumed there. The other phases contribute negligibly to the total lifetime of slightly less than 6 million years, except in the case of no neutrino emission. In that case, oxygen burning to iron lasts a period comparable with the helium burning lifetime.

The evolution of the star has been plotted on the theoretical H-R diagram in Figure 5. The shape of the track is very similar to the one computed for 15.6 $M_\odot$, except that at 30 $M_\odot$ the luminosity during helium burning increases very little.

The star sweeps out nearly the whole B spectral range during helium burning as a supergiant, from B8 to B1. By

the end of helium exhaustion, it passes quickly across the Hertzsprung Gap and becomes a K supergiant. Further gravitational contraction in the core is expected to bring the star into the region of the brightest M supergiants.

This work was supported by an NAS-NRC postdoctoral research associateship under the National Aeronautics and Space Administration. It is a pleasure to thank Dr. Robert Jastrow for his hospitality at the Institute for Space Studies.

REFERENCES

Allen, C. W. 1963, Astrophysical Quantities (London: Athlone Press).

Chandrasekhar, S. 1939, An Introduction to the Study of Stellar Structure (Chicago: University of Chicago Press).

Ezer, D., and Cameron, A. G. W. 1965, unpublished.

Fowler, W. A., and Hoyle, F. 1964, Ap. J. Suppl., 9, 201.

Hayashi, C., and Cameron, R. C. 1962, Ap. J., 136, 166.

Hayashi, C., Hoshi, R., and Sugimoto, D. 1962, Prog. Theoret. Phys. Suppl. (Kyoto), No. 22.

Hayashi, C., Jugaku, J., and Nishida, M. 1959, Prog. Theoret. Phys. (Kyoto), 22, 531.

———. 1960, Ap. J., 131, 241.

Iben, Jr., I. 1964, Ap. J., 140, 1631.

Reeves, H. 1963, Ap. J., 138, 79.

———. 1964, "On the Problem of Neon" (Goddard Institute for Space Studies, NASA Report).

———. 1965, Stars and Stellar Systems (Chicago: University of Chicago Press), Vol. 8, to be published.

Sakashita, S., Ôno, Y., and Hayashi, C. 1959, Prog. Theoret. Phys. (Kyoto), 22, 830.

Savedoff, M., and van Dyck, S. R. 1959, Modèles d'étoiles et évolution stellaire (extrait des Mém. Soc. Roy. Sci. Liège, Ser. 5, Vol. 3), p. 523.

Stein, R. 1965, "Stellar Evolution: A Survey with Analytic Models" (Goddard Institute for Space Studies, NASA Report).

Stothers, R. 1963a, Ap. J., 137, 770.

———. 1963b, ibid., 138, 1074 ("Paper I").

———. 1964, ibid., 140, 510 ("Paper II").

Tanaka, Y., and Sakashita, S. 1965, unpublished.

TABLE 1

Distribution of Chemical Composition in a Star of 30 $M_\odot$ during Helium Burning

Zone	I-phase	He-phase	X-phase
I	X_e	X_e	X_e
IIa	semiconvective	semiconvective	semiconvective
IIb	...	...	$X = X_s$
IIIa	$X = a_o+a_1q+a_2q^2$	$X = a_o+a_1q+a_2q^2$	$\mu = \mu_s(q/q_s)^{-\lambda}$
IIIb	$X = 0,\ Y = 1-Z_e$	$X = 0,\ Y = 1-Z_e$	$X = 0,\ Y = 1-Z_e$
IIIc	...	...	$X=0,\ Y\approx 0,\ Z=1$
IV	$Y = 1-Z_e$	$Y = Y_c,\ Z = 1-Y_c$	$Y \approx 0,\ Z = 1$

TABLE 2

Evolutionary Models of a Star of 30 $M_\odot$ during Helium Ignition (I) Phase*

	Models					
	1	2	3	4	5	6
log C	-3.145	-3.140	-3.137	-3.135	-3.133	-3.131
q_1	0.772	0.774	0.775	0.775	0.776	0.777
$q_2 \approx q_3$	0.461	0.456	0.453	0.451	0.449	0.447
β_s	0.455	0.448	0.444	0.441	0.438	0.436
log T_s	7.711	7.717	7.722	7.725	7.729	7.732
log ρ_s	0.656	0.663	0.669	0.674	0.680	0.687
log (r_s/R)	-1.968	-2.099	-2.185	-2.247	-2.312	-2.366
U_s	0.288	0.260	0.245	0.235	0.226	0.219
V_s	3.943	3.984	4.008	4.022	4.035	4.046
$(n+1)_s$	3.978	3.981	3.981	3.983	3.984	3.984
q_4	0.033	0.083	0.122	0.150	0.182	0.210
β_c	0.695	0.684	0.679	0.676	0.674	0.672
log T_c	8.243	8.256	8.262	8.265	8.267	8.269
log ρ_c	2.699	2.716	2.725	2.730	2.732	2.733
L_H/L	0.497	0.535	0.566	0.593	0.629	0.669
L_{He}/L	0.061	0.147	0.210	0.253	0.297	0.331
L_g/L	0.442	0.318	0.224	0.154	0.074	.....
log $(L/L_\odot)$	5.553	5.558	5.561	5.563	5.565	5.567
log $(R/R_\odot)$	1.792	1.905	1.981	2.035	2.092	2.139
log T_e	4.256	4.200	4.163	4.137	4.109	4.086
τ (10^4 years)	0.00	0.24	0.42	0.58	0.84	1.50

*Also, $q_s = 0.328$; $X_s = 0.018$; $\lambda_s = 1.552$; and $Y = 0.97$, $X_c = 0$ in the convective core.

TABLE 3

Evolutionary Models of a Star of 30 $M_\odot$ during Helium Depletion (He) Phase

	Models									
	1	2	3	4	5	6	7	8	9	10
log C	-3.135	-3.136	-3.135	-3.133	-3.132	-3.130	-3.127	-3.125	-3.123	-3.120
q_1	0.776	0.776	0.776	0.776	0.777	0.777	0.778	0.779	0.781	0.782
$q_2 = q_3$	0.449	0.449	0.449	0.448	0.447	0.445	0.443	0.442	0.441	0.440
X_2	0.475	0.477	0.476	0.474	0.473	0.472	0.470	0.470	0.471	0.474
X_3	0.348	0.350	0.349	0.346	0.342	0.338	0.332	0.328	0.325	.....
q_s	0.328	0.390	0.410	0.425	0.431	0.435	0.438	0.439	0.440	0.440
X_s	0.018	0.192	0.246	0.285	0.301	0.311	0.319	0.322	0.324	0.474
λ_s	1.552	1.349	1.299	1.266	1.253	1.244	1.238	1.236	1.234	.....
θ_s	0.441	0.450	0.450	0.446	0.440	0.432	0.419	0.409	0.395	0.386
log T_s	7.732	7.683	7.673	7.662	7.656	7.651	7.646	7.645	7.645	7.645
log ρ_s	0.694	0.456	0.396	0.337	0.300	0.265	0.224	0.201	0.175	0.093
log (r_s/R)	-2.346	-1.908	-1.771	-1.695	-1.683	-1.690	-1.724	-1.749	-1.792	-1.860
U_s	0.221	0.153	0.142	-0.130	0.121	0.110	0.0958	0.0871	0.0762	0.0573
V_s	4.102	3.852	3.745	3.654	3.615	3.585	3.558	3.529	3.486	3.027
$(n+1)_s$	3.985	3.986	4.001	4.037	4.071	4.116	4.185	4.243	4.323	3.917

TABLE 3 (Cont'd.)

q_4	0.210	0.279	0.306	0.332	0.345	0.354	0.363	0.366	0.370	0.371
Y	0.970	0.793	0.622	0.414	0.291	0.188	0.0974	0.0636	0.0297	0.0129
X_C	0.000	0.172	0.328	0.489	0.557	0.575	0.524	0.473	0.389	0.332
β_C	0.672	0.615	0.580	0.543	0.521	0.503	0.486	0.480	0.474	0.472
log T_C	8.269	8.289	8.306	8.329	8.349	8.369	8.398	8.416	8.441	8.467
log ρ_C	2.733	2.712	2.726	2.767	2.809	2.858	2.935	2.986	3.058	3.136
L_H/L	0.666	0.482	0.379	0.266	0.201	0.150	0.104	0.088	0.075	0.073
L_{He}/L	0.334	0.502	0.570	0.596	0.556	0.443	0.265	0.158	0.052	0.014
L_C/L	0.000	0.016	0.051	0.138	0.243	0.407	0.631	0.754	0.873	0.913
log $(L/L_\odot)$	5.564	5.563	5.563	5.565	5.567	5.569	5.572	5.573	5.576	5.578
log $(R/R_\odot)$	2.119	1.732	1.610	1.547	1.539	1.546	1.574	1.593	1.626	1.680
log T_e	4.095	4.288	4.349	4.381	4.386	4.383	4.369	4.360	4.344	4.318
τ (10^5 years)	0.00	0.91	1.71	2.69	3.29	3.84	4.42	4.68	4.98	5.16

TABLE 4

Evolutionary Models of a Star of 30 $M_\odot$ during Helium Exhaustion (X) Phase*

	Models				
	1	2	3	4	5
log C	-3.117	-3.114	-3.112	-3.100	-3.096
q_1	0.783	0.785	0.786	0.791	0.792
q_2	0.450	0.461	0.469	0.531	0.531
q_3	0.439	0.438	0.439	0.439	0.448
X_2	0.480	0.488	0.496	0.552	0.549
X_3	0.477	0.483	0.487	0.528	0.529
q_s	0.439	0.438	0.439	0.439	0.439
X_s	0.477	0.483	0.487	0.528	0.528
β_s	0.378	0.369	0.365	0.328	0.314
$\log(r_s/R)$	-1.965	-2.078	-2.146	-2.735	-3.614
U_s	0.0477	0.0398	0.0358	0.0159	0.0105
V_s	3.091	3.150	3.182	3.379	3.667
$(n+1)_s$	3.925	3.929	3.930	3.947	3.988
β_c	0.470	0.471	0.472	0.472	0.472
$\log(L/L_\odot)$	5.582	5.585	5.587	5.599	5.603
$\log(R/R_\odot)$	1.76	1.86	1.9	2.6	3.1
log T_e	4.28	4.23	4.2	3.9	3.6

*Also, q_α = 0.371; Y_α = 0.97; and μ = 2 below q_α.

TABLE 5

Evolutionary Timetable for a Star of 30 $M_{\odot}$

Phase	Lifetime (10^4 years)	Phase	Lifetime (10^4 years)
Pre-main-sequence contraction	2	Helium depletion (He)	51.6
Hydrogen burning (H)	480	Helium exhaustion (X)	1.3
Hydrogen exhaustion (E)	8.8	Gravitational (ν or no ν)	$\sim$ 1 or $\sim$ 3
Gravitational (G)	0.9	Oxygen to iron (ν or no ν)	$\sim$ 0 or $\sim$ 30
Helium ignition (I)	1.5	Total (ν or no ν)	547 or 579

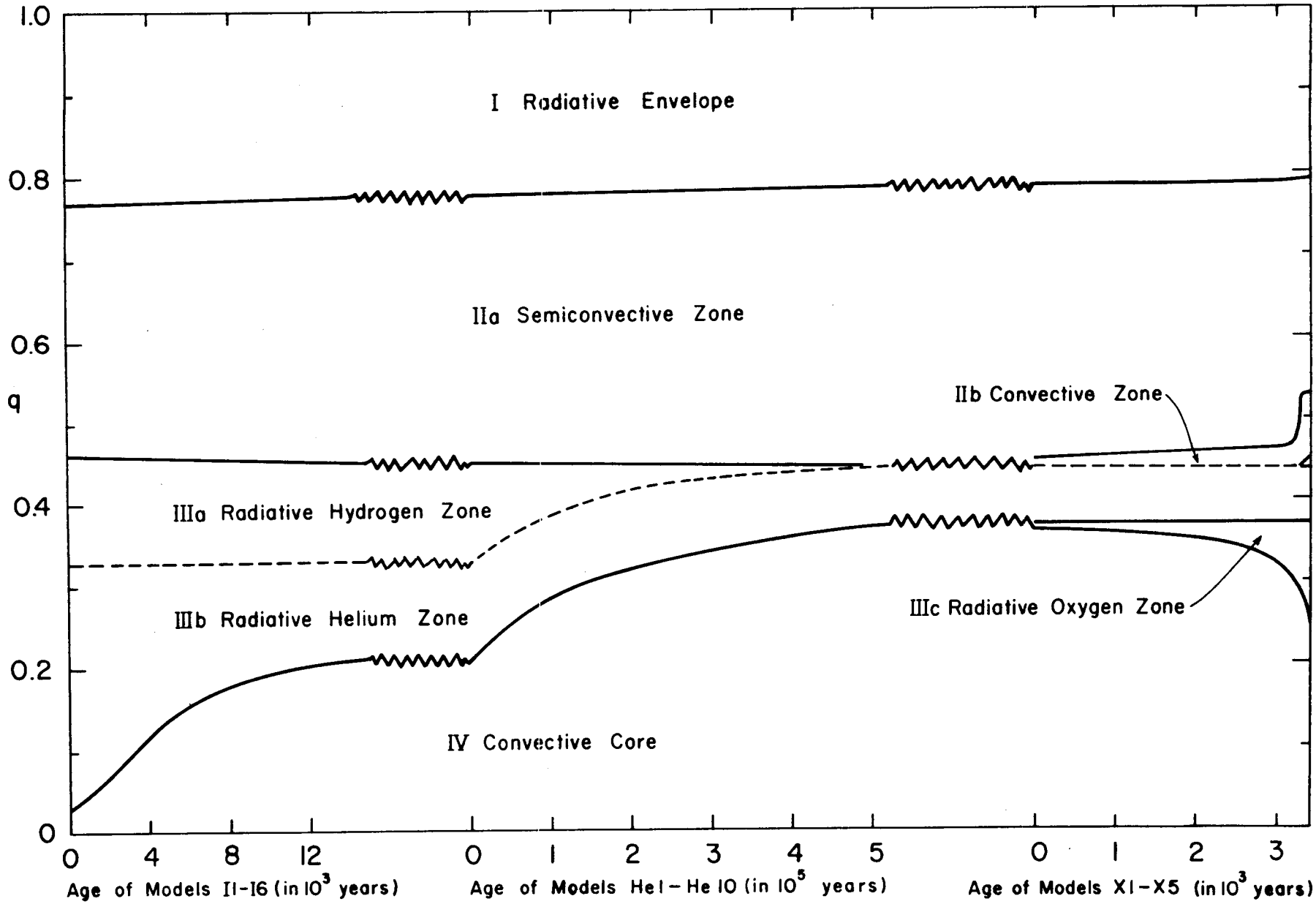
1.0
0.8
0.6
0.4
0.2
0
q
I Radiative Envelope
IIa Semiconvective Zone
IIb Convective Zone
IIIa Radiative Hydrogen Zone
IIIb Radiative Helium Zone
IIIc Radiative Oxygen Zone
IV Convective Core
0 4 8 12
Age of Models I1-16 (in 10^3 years)
0 1 2 3 4 5
Age of Models He1 - He 10 (in 10^5 years)
0 1 2 3
Age of Models X1 - X5 (in 10^3 years)

Fig. 1

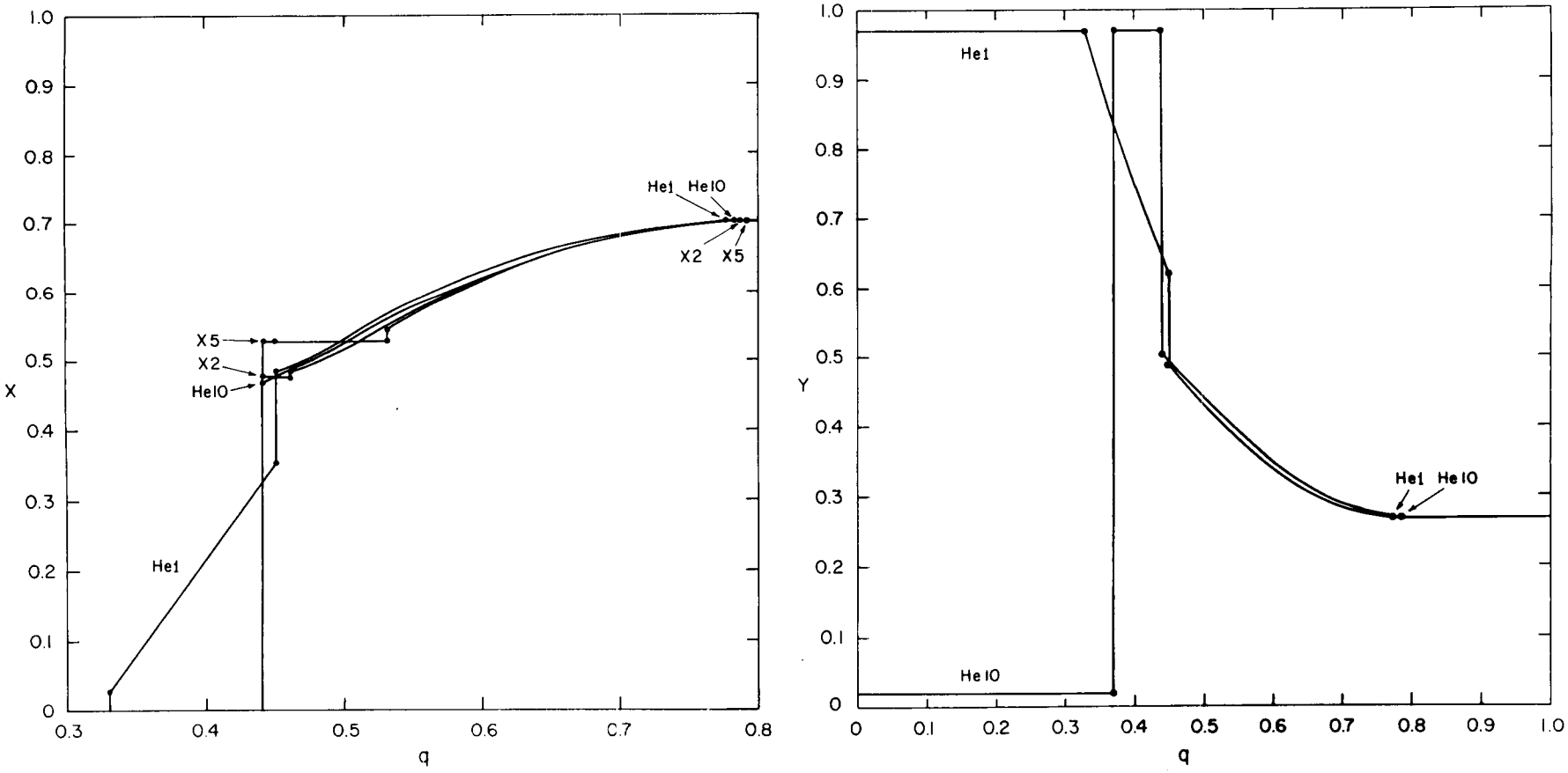

Fig. 2

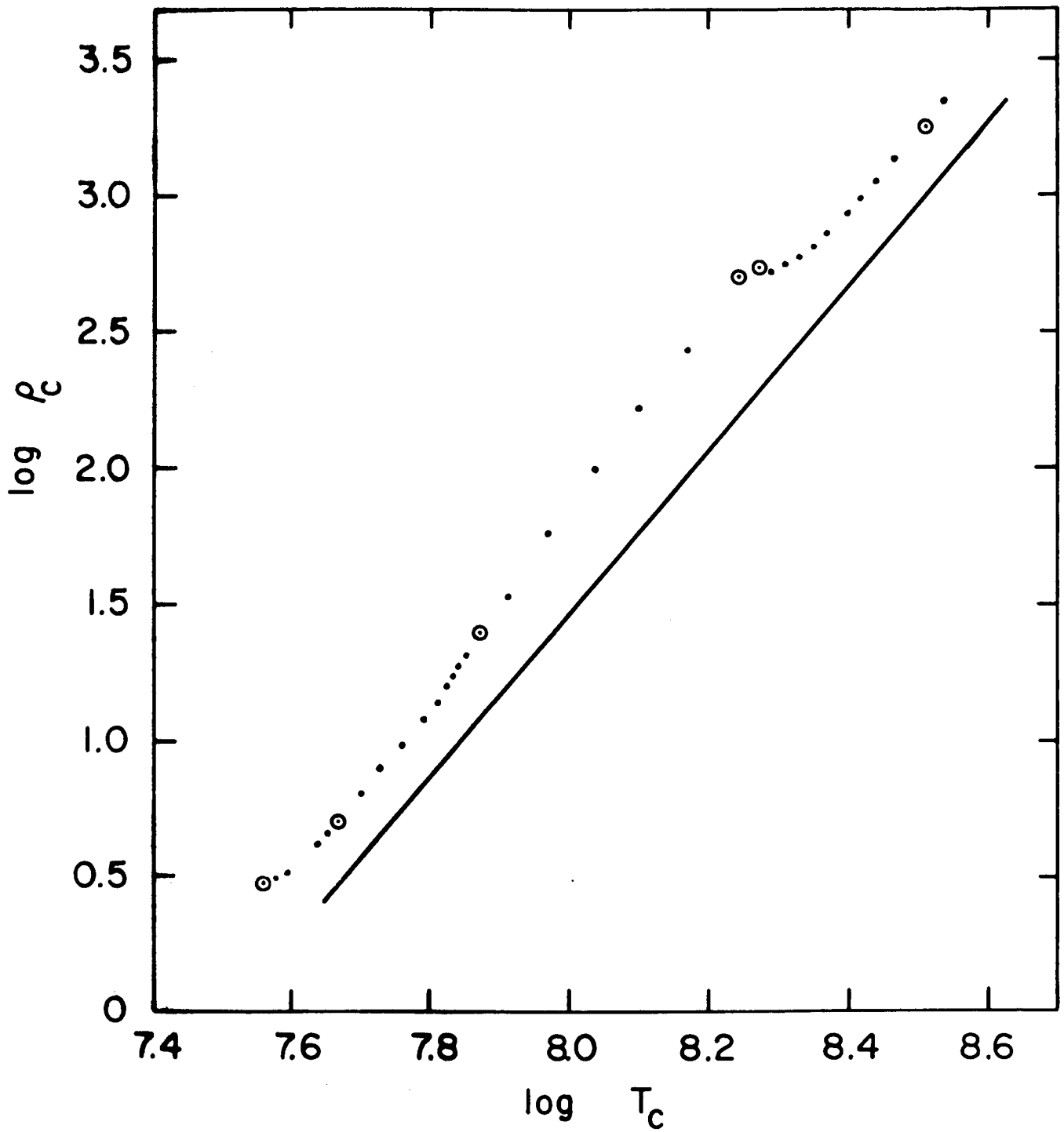

Fig. 3

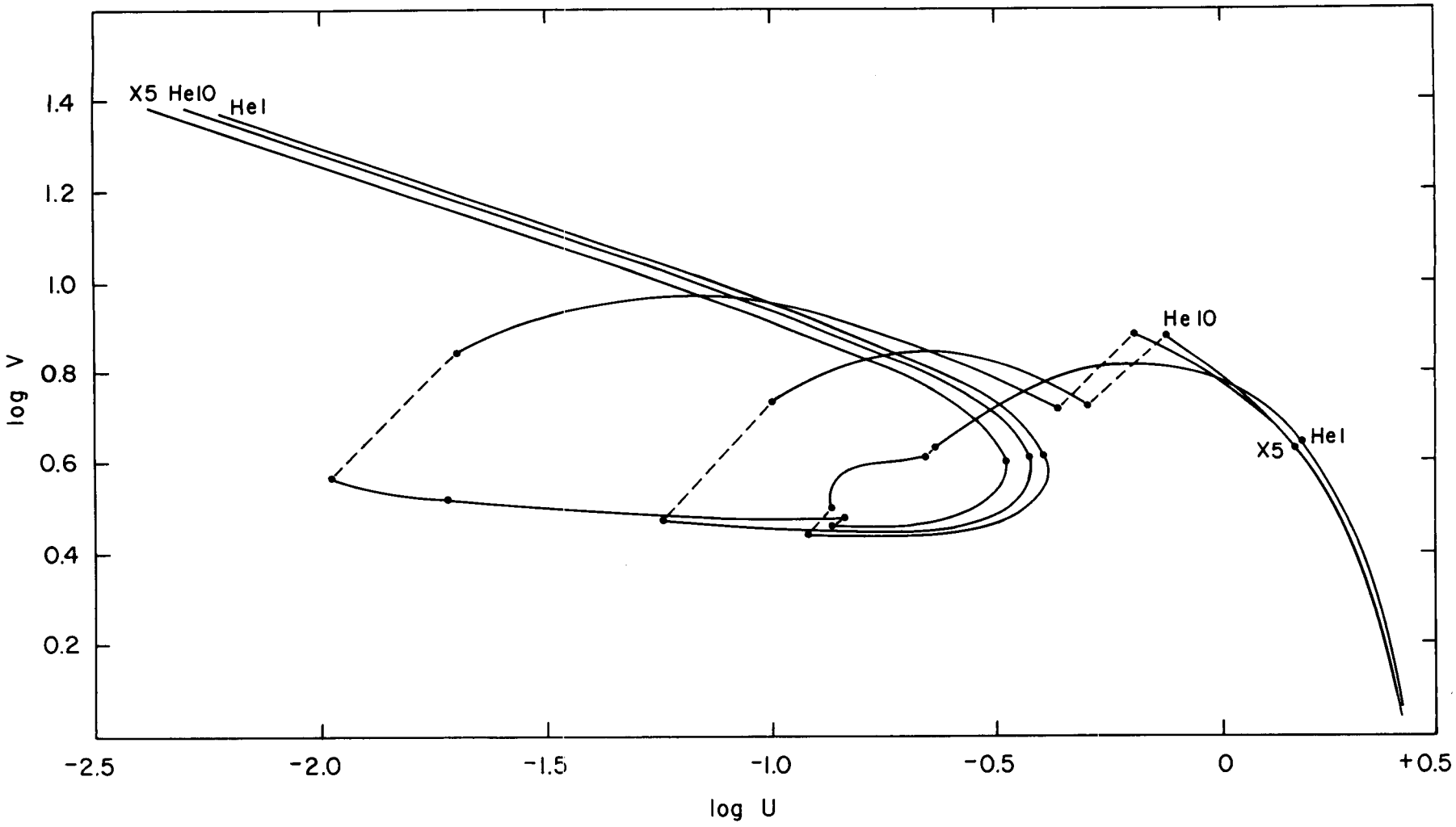
X5 HeIO
HeI
He IO
X5
HeI
log V
log U
1.4
1.2
1.0
0.8
0.6
0.4
0.2
-2.5
-2.0
-1.5
-1.0
-0.5
0
+0.5

Fig. 4

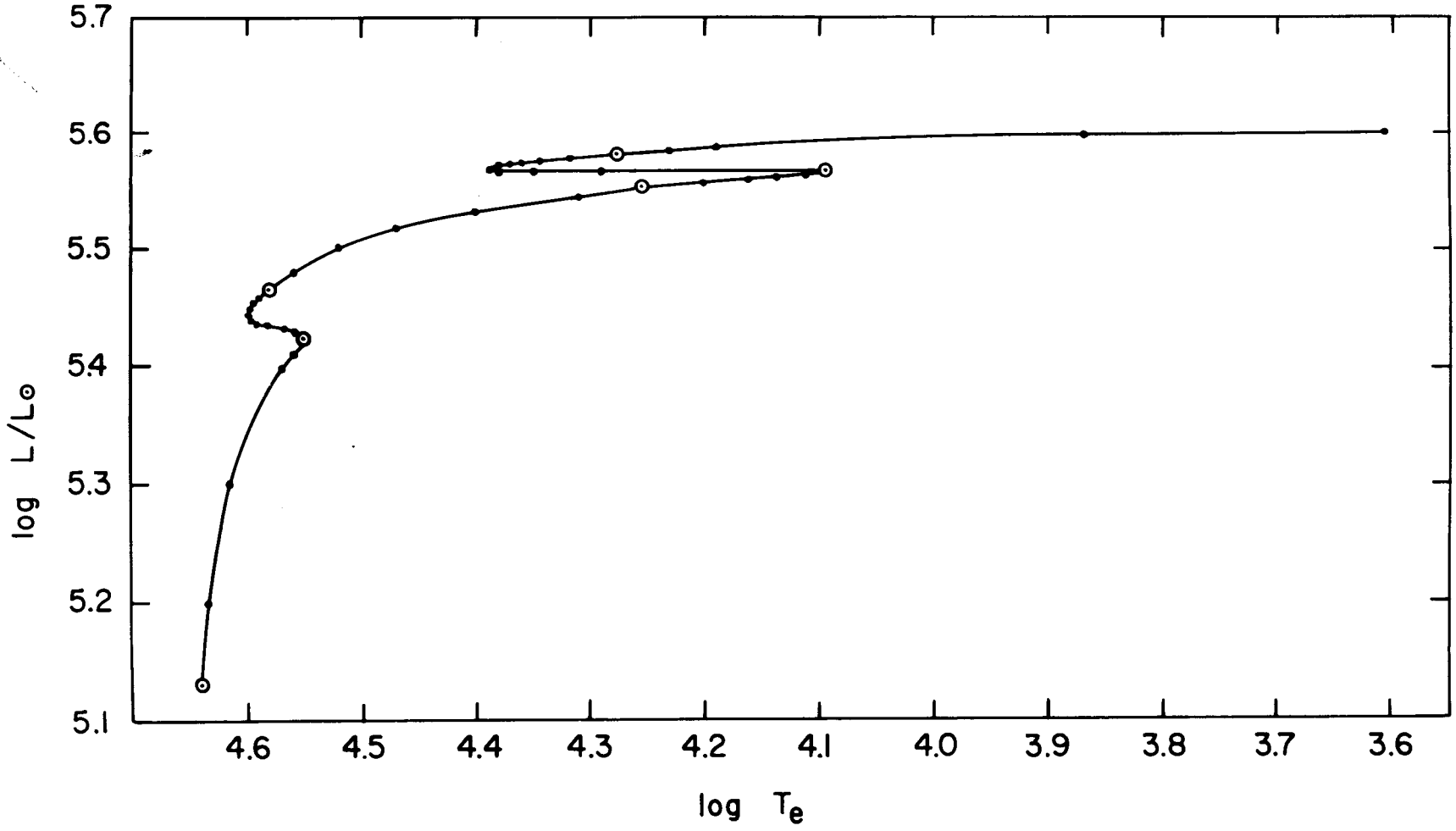

Fig. 5

FIGURE LEGENDS

Fig. 1. — Evolution of the structural zones of a star of 30 $M_\odot$ during the phases of helium ignition, depletion, and exhaustion.

Fig. 2a,b. — Distribution of hydrogen and helium as a function of mass fraction during the helium depletion (He) and exhaustion (X) phases. Dots represent zonal boundaries.

Fig. 3. — Evolution of the center of a star of 30 $M_\odot$ from the initial main sequence into helium exhaustion (Models H0-X2). Circles represent the first stages of the various phases. The line has a slope of 3.

Fig. 4. — Evolution of a star of 30 $M_\odot$ in the U-V plane, during the helium depletion (He) and exhaustion (X) phases. Dots represent zonal boundaries. Dashed lines refer to discontinuities in the chemical composition. Model X5 is based on the assumption that $q_g = q_s$.

Fig. 5. — Evolution of a star of 30 $M_\odot$ on a plot of luminosity versus effective temperature, from the initial main sequence through helium exhaustion. Circles represent the first stage of the various phases.